A Ritz type solution with exponential trial functions for laminated composite beams based on the modified couple stress theory

Ngoc-Duong Nguyen[a], Trung-Kien Nguyen[a,*], Huu-Tai Thai[b], Thuc P. Vo[c,d]

[a] Faculty of Civil Engineering, Ho Chi Minh City University of Technology and Education, 1 Vo Van Ngan Street, Thu Duc District, Ho Chi Minh City, Viet Nam.

[b] School of Engineering and Mathematical Sciences, La Trobe University, Bundoora, VIC 3086, Australia

[c] Institute of Research and Development, Duy Tan University, 03 Quang Trung, Da Nang, Vietnam

[d] Faculty of Engineering and Environment, Northumbria University, Newcastle upon Tyne, NE1 8ST, UK.

Abstract

This paper proposes novel Ritz functions for the size-dependent analysis of micro laminated composite beams with arbitrary lay-ups. Displacement field is based on a higher-order deformation beam theory and size effect is captured by the modified couple stress theory. Lagrange's equations are used to obtain the governing equations of motion. The present beam model, which can recover the classical one by neglecting the material length scale parameter, is used to predict the size-dependent responses of micro composite beams. The results indicate that the present study is efficient for bending, vibration and buckling problems of micro composite beams. Some new results are given to serve as benchmarks for future studies.

Keywords: Size-dependent behaviour; Ritz method; Bending; Vibration; Buckling; Micro composite beams.

* Corresponding author. Tel.: + 848 3897 2092.
E-mail address: kiennt@hcmute.edu.vn (Trung-Kien Nguyen)

1. Introduction

Composite materials are commonly used in many engineering fields because they have many advantages such as high stiffness-to-weight and strength-to-weight ratios as well as the ability to change fibre orientations or density to meet design requirements. In addition to their extensive use in practice, composite materials also attract many academic researchers [1-14]. In these studies, classical continuum theories are used to analyse macro composite beams. It should be noted that the classical continuum theories are unable to capture size effects. The experiment works made by Stolken and Evans [15] and Fleck et al. [16] indicated that the behaviour of microstructures is size-dependent.

A review of non-classical continuum mechanics models for size-dependent analysis of small-scale structures can be found in [17]. These models for size-dependent analysis can be divided into three groups: nonlocal elasticity theory, micro continuum theory and strain gradient family. Nonlocal elasticity theory was proposed by Eringen [18, 19], Eringen and Edelen [20], and its recent applications can be found in [21-24]. In this theory, the stress at a reference point is considered as a function of strain field at all points of the body, and thus the size effect is captured by means of constitutive equations using a nonlocal parameter. Micro continuum theory in which each particle can rotate and deform independently regardless of the motion of the centroid of the particle was developed by Eringen [25-27]. The strain gradient family is composed of the strain gradient theory [16, 28], the modified strain gradient theory [29], the couple stress theories [30-32] and the modified couple stress theory (MCST) [33]. In the strain gradient family, both strains and gradient of strains are considered in the strain energy. The size effect is accounted for using material length scale parameters (MLSP). The

MCST introduced an equilibrium condition of moments of couples to enforce the couple stress tensor to be symmetric. Consequently, MCST needs only one MLSP instead of two as the couple stress theories, or three as the modified strain gradient theory. This feature makes the MCST easier to use and more preferable to capture the size effect because the determination of MLSP is a challenging task.

Chen et al. [34, 35] developed Timoshenko and Reddy beam models to analyse the static behaviours of cross-ply simply supported microbeams. Chen and Si [36] suggested an anisotropic constitutive relation for the MCST and used global-local theory to analyse Reddy beams using Navier solutions. By using a meshless method, Roque et al. [37] analysed the static bending response of micro laminated Timoshenko beams. A size-dependent zigzag model was also proposed by Yang et al. [38] for the bending analysis of cross-ply microbeams. Abadi and Daneshmehr [39] analysed the buckling of micro composite beams using Euler-Bernoulli and Timoshenko models. Mohammadabadi et al. [40] also predicted the thermal effect on size-dependent buckling behaviour of micro composite beams. The generalized differential quadrature method was used to solve with different boundary conditions (BCs). Chen and Li [41] predicted dynamic behaviours of micro laminated Timoshenko beams. Mohammad-Abadi and Daneshmehr [42] used the MCST to analyse free vibration of cross-ply microbeams by using Euler-Bernoulli, Timoshenko and Reddy beam models. Ghadiri et al. [43] analysed the thermal effect on dynamics of thin and thick microbeams with different BCs. Most of the above-mentioned studies mainly focused on cross-ply microbeams. Therefore, the study of micro general laminated composite beams (MGLCB) with arbitrary lay-ups is necessary.

Despite in fact that numerical approaches are used increasingly [6, 21, 22, 37, 44, 45],

Ritz method is still efficient to analyse structural behaviours of beams [3, 4, 12, 13, 46-49]. In Ritz method, the accuracy and efficiency of solution strictly depends on the choice of trial functions. An inappropriate choice of the trial functions may cause slow convergence rates and numerical instabilities [13]. The trial functions should satisfy the specified essential BCs [50]. If this requirement is not satisfied, the Lagrangian multipliers and penalty method can be used to handle arbitrary BCs [4, 14, 51]. However, this approach leads to an increase in the dimension of the stiffness and mass matrices and causing computational costs. Therefore, the objective of this study is to propose trial functions for Ritz type solutions that give fast convergence rate, numerical stability and satisfy the specified BCs.

In this study, new exponential trial functions are proposed for the size-dependent analysis of MGLCB based on the MCST using a refined shear deformation theory. Lagrange's equations are used to obtain the governing equations of motion. The accuracy of the present model is demonstrated by verification studies. Numerical results are presented to investigate the effects of MLSP, span-to-thickness ratio and fibre angle on the deflections, stresses, natural frequencies and critical buckling loads of micro composite beams with arbitrary lay-ups.

2. Theoretical formulation

A MGLCB with rectangular cross-section shown in Fig. 1 is considered. L, b and h denote are the length, width and thickness of the beam, respectively. It is composed of n plies of orthotropic materials in different fibre angles with respect to the x-axis.

2.1. Kinematics

The beam theory based on refined shear deformation plate theory ([52, 53]). The displacement field accounts a higher-order variation of axial displacement and meets the

traction-free boundary conditions of the transvese shear stress on the top and bottom surfaces of the beams:

$$u(x,z,t)=u_0(x,t)-z\frac{\partial w_0(x,t)}{\partial x}+\left(\frac{5z}{4}-\frac{5z^3}{3h^2}\right)\beta_0(x,t)=u_0(x,t)-zw_{0,x}+f(z)\beta_0(x,t) \quad (1a)$$

$$v(x,z,t)=0 \quad (1b)$$

$$w(x,z,t)=w_0(x,t) \quad (1c)$$

where $u_0(x,t)$ and $w_0(x,t)$ are the axial and transverse displacements of a point on the beam mid-plane along the x- and z-directions, respectively; $\beta_0(x,t)$ is the rotation of the cross-section about the *y*-axis and $f(z)=\frac{5z}{4}-\frac{5z^3}{3h^2}$ is the shape function. The comma indicates a partial differentiation with respect to the corresponding subscript coordinate.

Based on the MCST [33], the rotation about the x-, y-, z-axes are determined by:

$$\theta_x(x,z,t)=\frac{1}{2}\left(w_{,y}-v_{,z}\right)=0 \quad (2a)$$

$$\theta_y(x,z,t)=\frac{1}{2}\left(u_{,z}-w_{,x}\right)=\frac{1}{2}\left(f_{,z}\beta_0-2w_{0,x}\right) \quad (2b)$$

$$\theta_z(x,z,t)=\frac{1}{2}\left(v_{,x}-u_{,y}\right)=0 \quad (2c)$$

The strain and curvature fields of beams are obtained as:

$$\varepsilon_x=\frac{\partial u}{\partial x}=u_{0,x}-zw_{0,xx}+f\beta_{0,x} \quad (3a)$$

$$\gamma_{xz}=\frac{\partial u}{\partial z}+\frac{\partial w}{\partial x}=f_{,z}\beta_0 \quad (3b)$$

$$\chi_{xy}=\frac{\partial \theta_y}{\partial x}=\frac{1}{2}\left(f_{,z}\beta_{0,x}-2w_{0,xx}\right) \quad (3c)$$

$$\chi_{zy} = \frac{\partial \theta_y}{\partial z} = \frac{1}{2} f_{,zz} \beta_0 \tag{3d}$$

2.2. Constitutive relations

The stress-strain relation for the k^{th}-ply of a laminated beam in global coordinate system is expressed as [5]:

$$\begin{Bmatrix} \sigma_x \\ \sigma_z \\ \sigma_{xz} \end{Bmatrix}^k = \begin{pmatrix} \bar{\bar{Q}}_{11} & \bar{\bar{Q}}_{13} & 0 \\ \bar{\bar{Q}}_{13} & \bar{\bar{Q}}_{33} & 0 \\ 0 & 0 & \bar{\bar{Q}}_{55} \end{pmatrix}^k \begin{Bmatrix} \varepsilon_x \\ \varepsilon_z \\ \gamma_{xz} \end{Bmatrix} \tag{4}$$

where $\bar{\bar{Q}}_{11}$, $\bar{\bar{Q}}_{13}$, $\bar{\bar{Q}}_{33}$, $\bar{\bar{Q}}_{55}$ are elastic stiffness coefficients in the global coordinate system which can be found in [5] for details. When the transversely normal stress is neglected ($\sigma_z = 0$), the strain-stress relation is written as:

$$\begin{Bmatrix} \sigma_x \\ \sigma_{xz} \end{Bmatrix}^{(k)} = \begin{pmatrix} \bar{\bar{Q}}^*_{11} & 0 \\ 0 & \bar{\bar{Q}}^*_{55} \end{pmatrix}^{(k)} \begin{Bmatrix} \varepsilon_x \\ \gamma_{xz} \end{Bmatrix} \tag{5}$$

where:

$$\bar{\bar{Q}}^*_{11} = \bar{\bar{Q}}_{11} - \frac{\bar{\bar{Q}}^2_{13}}{\bar{\bar{Q}}_{33}}, \quad \bar{\bar{Q}}^*_{55} = \bar{\bar{Q}}_{55} \tag{6}$$

The couple stress-curvature relation for the k^{th}-ply of a laminated beam can be given by [40]:

$$\begin{Bmatrix} m_{xy} \\ m_{zy} \end{Bmatrix}^k = \begin{bmatrix} \bar{\bar{Q}}^*_{44} & 0 \\ 0 & \bar{\bar{Q}}^*_{66} \end{bmatrix}^k \begin{Bmatrix} \chi_{xy} \\ \chi_{zy} \end{Bmatrix} \tag{7}$$

where:

$$\bar{\bar{Q}}^*_{44} = \xi^2_{kb} C_{55} m^2 \left(m^2 - n^2\right) - \xi^2_{km1} C_{44} n^2 \left(m^2 - n^2\right) + 2m^2 n^2 \left(\xi^2_{kb} C_{44} + \xi^2_{km1} C_{55}\right) \tag{8a}$$

$$\bar{\bar{Q}}^*_{66} = \xi^2_{km2} \left(C_{55} m^2 + C_{44} n^2\right) \tag{8b}$$

In the above formulas, C_{ij} are elastic coefficients of orthotropic material [50]; ξ_{kb}, ξ_{km1} and ξ_{km2} are respectively the MLSPs in x'-, y'- and z-directions. In term of physical meaning, ξ_{kb} represents the micro-scale material parameter of the fiber rotating in the $y'-z$ plane where the fiber cross-section and the matrix interact, and the fiber are viewed as the impurity affecting the rotational equilibrium. ξ_{km1} and ξ_{km2} represent the micro-scale material parameter within the matrix rotating about the impurity in the $x'-z$ and $x'-y'$ plane, respectively [32, 41]; $m=\cos\psi^k$, $n=\sin\psi^k$, ψ^k is a fiber angle with respect to the x-axis.

2.3. Variational formulation

The strain energy, work done and kinetic energy are denoted by U, V and K respectively. The strain energy U of the beam is given by:

$$\begin{aligned} U &= \frac{1}{2}\int_V \left(\sigma_x\varepsilon_x+\sigma_{xz}\gamma_{xz}+m_{xy}\chi_{xy}+m_{zy}\chi_{zy}\right)dV \\ &= \frac{1}{2}\int_0^L \Big[A\left(u_{0,x}\right)^2 - 2Bu_{0,x}w_{0,xx} + 2B^s u_{0,x}\beta_{0,x} + \left(A^m+D\right)\left(w_{0,xx}\right)^2 \\ &\quad -2\left(\frac{B^m}{2}+D^s\right)w_{0,xx}\beta_{0,x} + \left(\frac{D^m}{4}+H^s\right)(\beta_{0,x})^2 + \left(A^s+\frac{H^m}{4}\right)(\beta_0)^2 \Big] dx \end{aligned} \tag{9}$$

where the stiffness coefficients of the beam are determined as follows:

$$\left(A,B,D,B^s,D^s,H^s\right)=\sum_{k=1}^{n}\int_{z_k}^{z_{k+1}}\bar{\bar{Q}}_{11}^{*}\left(1,z,z^2,f,zf,f^2\right)bdz \tag{10a}$$

$$A^s=\sum_{k=1}^{n}\int_{z_k}^{z_{k+1}}\bar{\bar{Q}}_{55}^{*}f_{,z}^2bdz \tag{10b}$$

$$\left(A^m,B^m,D^m\right)=\sum_{k=1}^{n}\int_{z_k}^{z_{k+1}}\bar{\bar{Q}}_{44}^{*}\left(1,f_{,z},f_{,z}^2\right)bdz \tag{10c}$$

$$H^m=\sum_{k=1}^{n}\int_{z_k}^{z_{k+1}}\bar{\bar{Q}}_{66}^{*}f_{,zz}^2bdz \tag{10d}$$

The work done V by axially compressive load N_0 and transverse load q is given by:

$$V = \frac{1}{2}\int_0^L N_0 (w_{0,x})^2 b dx - \int_0^L q w_0 b dx \tag{11}$$

The kinetic energy K of the beam is written by:

$$K = \frac{1}{2}\int_V \rho(z)\left(\dot{u}^2 + \dot{v}^2 + \dot{w}^2\right) dV$$

$$= \frac{1}{2}\int_0^L \left[I_0 \dot{u}_0^2 - 2I_1 \dot{u}_0 \dot{w}_{0,x} + I_2 \left(\dot{w}_{0,x}\right)^2 + 2J_1 \dot{\beta}_0 \dot{u}_0 - 2J_2 \dot{\beta}_0 \dot{w}_{0,x} + K_2 \dot{\beta}_0^2 + I_0 \dot{w}_0^2 \right] dx \tag{12}$$

where the dot-superscript denotes the differentiation with respect to the time t; ρ is the mass density of each layer; I_0, I_1, I_2, J_1, J_2, K_2 are the inertia coefficients determined by:

$$\left(I_0, I_1, I_2, J_1, J_2, K_2\right) = \sum_{k=1}^{n} \int_{z_k}^{z_{k+1}} \rho^{(k)} \left(1, z, z^2, f, zf, f^2\right) b dz \tag{13}$$

The total potential energy of system is expressed by:

$$\Pi = U + V - K$$

$$\Pi = \frac{1}{2}\int_0^L \left[A\left(u_{0,x}\right)^2 - 2B u_{0,x} w_{0,xx} + 2B^s u_{0,x} \beta_{0,x} + \left(A^m + D\right)\left(w_{0,xx}\right)^2 - 2\left(\frac{B^m}{2} + D^s\right) w_{0,xx} \beta_{0,x} \right.$$
$$\left. + \left(\frac{D^m}{4} + H^s\right)(\beta_{0,x})^2 + \left(A^s + \frac{H^m}{4}\right)(\beta_0)^2 \right] dx + \frac{1}{2}\int_0^L N_0 (w_{0,x})^2 b dx - \int_0^L q w_0 b dx \tag{14}$$
$$- \frac{1}{2}\int_0^L \left[I_0 \dot{u}_0^2 - 2I_1 \dot{u}_0 \dot{w}_{0,x} + I_2 \left(\dot{w}_{0,x}\right)^2 + 2J_1 \dot{\beta}_0 \dot{u}_0 - 2J_2 \dot{\beta}_0 \dot{w}_{0,x} + K_2 \dot{\beta}_0^2 + I_0 \dot{w}_0^2 \right] dx$$

2.4. Ritz solution

By using Ritz method, the displacement field in Eq. (14) is approximated by:

$$u_0(x,t) = \sum_{j=1}^{m} \varphi_{j,x}(x) u_j e^{i\omega t} \tag{15a}$$

$$w_0(x,t)=\sum_{j=1}^{m}\varphi_j(x)w_j e^{i\omega t} \tag{15b}$$

$$\beta_0(x,t)=\sum_{j=1}^{m}\varphi_{j,x}(x)\beta_j e^{i\omega t} \tag{15c}$$

where ω is the frequency, $i^2=-1$ the imaginary unit; u_j, w_j and β_j are unknown and need to be determined; $\varphi_j(x)$ are trial functions. In this paper, new exponential trial functions for Ritz solution reported in Table 1 are proposed for three typical BCs. It is clear that they satisfy various BCs: simply-supported (S-S), clamped-free (C-F) and clamped-clamped (C-C).

By substituting Eq. (15) into Eq. (14) and using Lagrange's equations:

$$\frac{\partial\Pi}{\partial p_j}-\frac{d}{dt}\frac{\partial\Pi}{\partial\dot{p}_j}=0 \tag{16}$$

with p_j representing the values of $\left(u_j, w_j, \beta_j\right)$, the static, vibration and buckling behaviour of MGLCB can be obtained by solving the following equations:

$$\left(\begin{bmatrix}\mathbf{K}^{11} & \mathbf{K}^{12} & \mathbf{K}^{13}\\ {}^{T}\mathbf{K}^{12} & \mathbf{K}^{22} & \mathbf{K}^{23}\\ {}^{T}\mathbf{K}^{13} & {}^{T}\mathbf{K}^{23} & \mathbf{K}^{33}\end{bmatrix}-\omega^2\begin{bmatrix}\mathbf{M}^{11} & \mathbf{M}^{12} & \mathbf{M}^{13}\\ {}^{T}\mathbf{M}^{12} & \mathbf{M}^{22} & \mathbf{M}^{23}\\ {}^{T}\mathbf{M}^{13} & {}^{T}\mathbf{M}^{23} & \mathbf{M}^{33}\end{bmatrix}\right)\begin{Bmatrix}\mathbf{u_0}\\ \mathbf{w_0}\\ \boldsymbol{\beta}_\mathbf{0}\end{Bmatrix}=\begin{Bmatrix}\mathbf{0}\\ \mathbf{F}\\ \mathbf{0}\end{Bmatrix} \tag{17}$$

where the components of stiffness matrix **K** and mass matrix **M** are given by:

$$K_{ij}^{11}=A\int_0^L\varphi_{i,xx}\varphi_{j,xx}dx,\quad K_{ij}^{12}=-B\int_0^L\varphi_{i,xx}\varphi_{j,xx}dx,\quad K_{ij}^{13}=B^s\int_0^L\varphi_{i,xx}\varphi_{j,xx}dx,$$

$$K_{ij}^{22}=\left(A^m+D\right)\int_0^L\varphi_{i,xx}\varphi_{j,xx}dx+N_0\int_0^L\varphi_{i,x}\varphi_{j,x}dx,\quad K_{ij}^{23}=-\left(\frac{B^m}{2}+D^s\right)\int_0^L\varphi_{i,xx}\varphi_{j,xx}dx,$$

$$K_{ij}^{33}=\left(\frac{D^m}{4}+H^s\right)\int_0^L\varphi_{i,xx}\varphi_{j,xx}dx+\left(\frac{H^m}{4}+A^s\right)\int_0^L\varphi_{i,x}\varphi_{j,x}dx, M_{ij}^{11}=I_0\int_0^L\varphi_{i,x}\varphi_{j,x}dx,$$

$$M_{ij}^{12}=-I_1\int_0^L\varphi_{i,x}\varphi_{j,x}dx, M_{ij}^{13}=J_1\int_0^L\varphi_{i,x}\varphi_{j,x}dx, M_{ij}^{22}=I_0\int_0^L\varphi_i\varphi_j dx+I_2\int_0^L\varphi_{i,x}\varphi_{j,x}dx,$$

$$M_{ij}^{23} = -J_2 \int_0^L \varphi_{i,x} \varphi_{j,x} dx, \quad M_{ij}^{33} = K_2 \int_0^L \varphi_{i,x} \varphi_{j,x} dx, \quad F_i = \int_0^L q \varphi_i dx. \tag{18}$$

3. Numerical results

3.1. Convergence and accuracy studies

Convergence and verification studies are conducted to demonstrate the accuracy of the present study. Laminates, which are made of the same orthotropic materials, have equal thicknesses with material properties in Table 2. The beam is under a uniformly distributed load $q = q_0$ or a sinusoidal load $q = q_0 \sin\left(\frac{\pi x}{L}\right)$. Unless otherwise stated, the following non-dimensional terms are used:

$$\bar{w} = \frac{100 w_0 E_2 b h^3}{q_0 L^4}, \quad \bar{\sigma}_x = \frac{b h^2}{q_0 L^2} \sigma_x \left(\frac{L}{2}, z\right), \quad \bar{\sigma}_{xz} = \frac{b h}{q_0 L} \sigma_{xz}(0, z), \quad \bar{N}_{cr} = N_{cr} \frac{L^2}{E_2 b h^3} \tag{19a}$$

$$\bar{\omega} = \frac{\omega L^2}{h} \sqrt{\frac{\rho}{E_2}} \text{ for Material (MAT) I and } \bar{\omega} = \frac{\omega L^2}{h} \sqrt{\frac{\rho}{E_1}} \text{ for MAT III} \tag{19b}$$

The numerical results of marco composite beams can be achieved by setting $\xi_{kb} = \xi_{km1} = \xi_{km2} = 0$. It should be noted that turning the composite laminated beam around the fiber direction is easier than turning around the normal to the fiber direction. The MLSP in the fiber direction is greater than that in other directions, i.e. $\xi_{kb} >> (\xi_{km1}, \xi_{km2})$. Therefore, only the MLSP in the fiber direction is considered in this study, i.e. $(\xi_{kb} = \xi_b)$ and $\xi_{km1} = \xi_{km2} = 0$. The value of the MLSP is referred from [34, 38-40, 42, 43].

Composite beams (MAT I, $0^0/90^0/0^0$, $L/h = 5$) with various BCs are considered to evaluate the convergence. The non-dimensional fundamental frequencies, critical buckling loads and mid-span displacements with respect to the series number m are

given in Table 3. The results indicate that $m=6$ is the convergence point for natural frequency, critical buckling load and displacement, respectively. Thus, this number of series terms is used hereafter. It can be stated that the convergence of present solution appears to be faster than that of the solution from [12] ($m=12$). This is advantage of proposed trial function.

In order to verify the accuracy of the present solution, the simply supported beams are investigated. Since there is no published data for the micro composite beams with arbitrary lay-ups, the verifications are only focused on cross-ply beams. The critical buckling loads and fundamental frequencies of $\left(90^0/0^0/90^0\right)$ and $\left(0^0/90^0/0^0\right)$ beams (MAT I) with $\xi_b=h$ are shown in Figs. 2 and 3, and compared with those from analytical solution of Abadi and Daneshmehr [39], Mohammad-Abadi and Daneshmehr [42]. It can be seen that the present results are in good agreements with previous results for Timoshenko and Reddy beam models.

Further verification is illustrated in Fig. 4 for $\left(90^0/0^0/90^0\right)$ beams (MAT II) with $\xi_b=h$ and L=4h, subjected to sinusoidal loads $q=q_0\sin\left(\frac{\pi x}{L}\right)$. It should be noted that the non-dimensional forms of the displacement and axial stress are $\bar{w}=100w_0E_2bh^3/q_0L^4$ and $\bar{\sigma}_x=\sigma_x\left(\frac{L}{2},z\right)/q_0$, respectively. There is a slight discrepancy between the present results and those of Yang et al. [38].

3.2. Static analysis

The static behaviours of the MGLCB with various BCs and span-to-thickness ratios are considered in this section. The non-dimensional mid-span displacements of beams (MAT II) subjected to a uniformly load $\left(q=q_0\right)$ with $\xi_b=0,\ h/4,\ h/2,\ h$ are shown

in Tables 4-6. It can be seen that the displacements of beams decrease as ξ_b increases for all BCs and span-to-thickness ratios. In the case of $\xi_b = 0,$ the results of marco beams are recovered and agree well with those of Vo et al. [1], which obtained from finite element model and higher-order beam theory.

In the next example, micro composite beams under sinusoidal loads, $q = q_0 \sin\left(\frac{\pi x}{L}\right)$ (MAT II, $L/h = 4$), are investigated. Their deflections with various MLSP are plotted in Figs. 5-7. It can be seen that they decrease with the increase of ξ_b. Fig. 8 shows mid-span displacements of $\left(0^0/30^0/0^0\right)$ and $\left(0^0/30^0\right)$ beams with different BCs. It is interesting to see that as ξ_b/h increases, the variation of the beams' displacement depends on BCs. The C-F beam has the biggest variation. The axial and shear stresses of $\left(0^0/60^0/0^0\right)$ and $\left(0^0/60^0\right)$ simply supported beams are shown in Figs. 9 and 10. Similar to the displacement, the stress also reduces as the MLSP increases.

3.3. Vibration and buckling analysis

The non-dimensional fundamental frequencies and critical buckling loads of the MGLCB with various BCs and span-to-thickness are given in Tables 7-10. For macro composite beams $(\xi_b = 0),$ the present results again agree well with those of Vo et al. [2] and Chen et al. [7] (Tables 7 and 8). Some new results for micro composite beams are shown to serve as benchmarks for future studies. It can be seen that the results are increased as ξ_b increases. This response can be expected because an increase in the MLSP leads to an increase in the beams' stiffness.

Figs. 11 and 12 show variation of the natural frequencies and critical buckling loads with respect to ξ_b/h ratio of $\left(0^0/30^0/0^0\right)$ and $\left(0^0/30^0\right)$ beams. It is clear that as

ξ_b / h increases, their variation depend on BCs. The C-C beam has the biggest variation. Fig. 13 shows first three mode shapes of $\left(0^0/45^0/0^0\right)$ and $\left(0^0/45^0\right)$ C-F beams. It can be seen that for unsymmetric beams, the bending mode w_0, axial mode u_0 and rotation mode β_0 are the dominate modes, which is different from that of symmetric ones.

4. Conclusions

The size effect, which is included by the modified couple stress theory, on bending, vibration and buckling behaviours of micro composite beams with arbitrary lay-ups is investigated in this study. The governing equations of motion are derived from Lagrange's equations. New trial functions are developed to solve problems. The frequencies, critical buckling loads, displacements and stresses of micro composite beams with various BCs are obtained. The results indicate that the present study is efficiency for predicting behaviours of micro laminated composite beams with arbitrary lay-ups.

Acknowledgements

This research is funded by Vietnam National Foundation for Science and Technology Development (NAFOSTED) under Grant No. 107.02-2015.07.

References

1. Vo T.P., Thai H.-T., Nguyen T.-K., Lanc D., and Karamanli A., *Flexural analysis of laminated composite and sandwich beams using a four-unknown shear and normal deformation theory.* Composite Structures, 2017. **176**(Supplement C): p. 388-397.
2. Vo T.P., Thai H.-T., and Aydogdu M., *Free vibration of axially loaded composite beams using a four-unknown shear and normal deformation theory.* Composite

Structures, 2017. **178**(Supplement C): p. 406-414.

3. Nguyen T.-K., Nguyen N.-D., Vo T.P., and Thai H.-T., *Trigonometric-series solution for analysis of laminated composite beams.* Composite Structures, 2017. **160**: p. 142-151.
4. Mantari J. and Canales F., *Free vibration and buckling of laminated beams via hybrid Ritz solution for various penalized boundary conditions.* Composite Structures, 2016. **152**: p. 306-315.
5. Li J., Huo Q., Li X., Kong X., and Wu W., *Vibration analyses of laminated composite beams using refined higher-order shear deformation theory.* International Journal of Mechanics and Materials in Design, 2014. **10**(1): p. 43-52.
6. Vo T.P. and Thai H.-T., *Vibration and buckling of composite beams using refined shear deformation theory.* International Journal of Mechanical Sciences, 2012. **62**(1): p. 67-76.
7. Chen W., Lv C., and Bian Z., *Free vibration analysis of generally laminated beams via state-space-based differential quadrature.* Composite Structures, 2004. **63**(3): p. 417-425.
8. Zenkour A.M., *Transverse shear and normal deformation theory for bending analysis of laminated and sandwich elastic beams.* Mechanics of Composite Materials and Structures, 1999. **6**(3): p. 267-283.
9. Khdeir A. and Reddy J., *An exact solution for the bending of thin and thick cross-ply laminated beams.* Composite Structures, 1997. **37**(2): p. 195-203.
10. Khdeir A. and Reddy J., *Buckling of cross-ply laminated beams with arbitrary boundary conditions.* Composite Structures, 1997. **1**(37): p. 1-3.
11. Chandrashekhara K., Krishnamurthy K., and Roy S., *Free vibration of composite*

beams including rotary inertia and shear deformation. Composite Structures, 1990. **14**(4): p. 269-279.

12. Nguyen N.-D., Nguyen T.-K., Nguyen T.-N., and Thai H.-T., *New Ritz-solution shape functions for analysis of thermo-mechanical buckling and vibration of laminated composite beams.* Composite Structures, 2018. **184**: p. 452-460.
13. Aydogdu M., *Buckling analysis of cross-ply laminated beams with general boundary conditions by Ritz method.* Composites Science and Technology, 2006. **66**(10): p. 1248-1255.
14. Canales F. and Mantari J., *Buckling and free vibration of laminated beams with arbitrary boundary conditions using a refined HSDT.* Composites Part B: Engineering, 2016. **100**: p. 136-145.
15. Stölken J. and Evans A., *A microbend test method for measuring the plasticity length scale.* Acta Materialia, 1998. **46**(14): p. 5109-5115.
16. Fleck N., Muller G., Ashby M., and Hutchinson J., *Strain gradient plasticity: theory and experiment.* Acta Metallurgica et Materialia, 1994. **42**(2): p. 475-487.
17. Thai H.-T., Vo T.P., Nguyen T.-K., and Kim S.-E., *A review of continuum mechanics models for size-dependent analysis of beams and plates.* Composite Structures, 2017. **177**(Supplement C): p. 196-219.
18. Eringen A.C., *Nonlocal polar elastic continua.* International journal of engineering science, 1972. **10**(1): p. 1-16.
19. Eringen A.C., *Linear theory of nonlocal elasticity and dispersion of plane waves.* International Journal of Engineering Science, 1972. **10**(5): p. 425-435.
20. Eringen A.C. and Edelen D., *On nonlocal elasticity.* International Journal of Engineering Science, 1972. **10**(3): p. 233-248.

21. Phung-Van P., Lieu Q.X., Nguyen-Xuan H., and Wahab M.A., *Size-dependent isogeometric analysis of functionally graded carbon nanotube-reinforced composite nanoplates.* Composite Structures, 2017. **166**: p. 120-135.
22. Phung-Van P., Ferreira A., Nguyen-Xuan H., and Wahab M.A., *An isogeometric approach for size-dependent geometrically nonlinear transient analysis of functionally graded nanoplates.* Composites Part B: Engineering, 2017. **118**: p. 125-134.
23. Nguyen N.-T., Kim N.-I., and Lee J., *Mixed finite element analysis of nonlocal Euler–Bernoulli nanobeams.* Finite Elements in Analysis and Design, 2015. **106**: p. 65-72.
24. Nguyen N.-T., Hui D., Lee J., and Nguyen-Xuan H., *An efficient computational approach for size-dependent analysis of functionally graded nanoplates.* Computer Methods in Applied Mechanics and Engineering, 2015. **297**: p. 191-218.
25. Eringen A.C., *Micropolar fluids with stretch.* International Journal of Engineering Science, 1969. **7**(1): p. 115-127.
26. Eringen A.C., *Linear theory of micropolar elasticity.* Journal of Mathematics and Mechanics, 1966: p. 909-923.
27. Eringen A.C., *Simple microfluids.* International Journal of Engineering Science, 1964. **2**(2): p. 205-217.
28. Mindlin R.D., *Second gradient of strain and surface-tension in linear elasticity.* International Journal of Solids and Structures, 1965. **1**(4): p. 417-438.
29. Lam D.C., Yang F., Chong A., Wang J., and Tong P., *Experiments and theory in strain gradient elasticity.* Journal of the Mechanics and Physics of Solids, 2003. **51**(8): p. 1477-1508.

30. Koiter W., *Couple-stresses in the theory of elasticity, I & II.* 1969.
31. Toupin R.A., *Elastic materials with couple-stresses.* Archive for Rational Mechanics and Analysis, 1962. **11**(1): p. 385-414.
32. Mindlin R. and Tiersten H., *Effects of couple-stresses in linear elasticity.* Archive for Rational Mechanics and analysis, 1962. **11**(1): p. 415-448.
33. Yang F., Chong A., Lam D.C., and Tong P., *Couple stress based strain gradient theory for elasticity.* International Journal of Solids and Structures, 2002. **39**(10): p. 2731-2743.
34. Wanji C., Chen W., and Sze K., *A model of composite laminated Reddy beam based on a modified couple-stress theory.* Composite Structures, 2012. **94**(8): p. 2599-2609.
35. Chen W., Li L., and Xu M., *A modified couple stress model for bending analysis of composite laminated beams with first order shear deformation.* Composite Structures, 2011. **93**(11): p. 2723-2732.
36. Chen W. and Si J., *A model of composite laminated beam based on the global–local theory and new modified couple-stress theory.* Composite Structures, 2013. **103**: p. 99-107.
37. Roque C., Fidalgo D., Ferreira A., and Reddy J., *A study of a microstructure-dependent composite laminated Timoshenko beam using a modified couple stress theory and a meshless method.* Composite Structures, 2013. **96**: p. 532-537.
38. Yang W., He D., and Chen W., *A size-dependent zigzag model for composite laminated micro beams based on a modified couple stress theory.* Composite Structures, 2017.
39. Abadi M.M. and Daneshmehr A., *An investigation of modified couple stress theory*

in buckling analysis of micro composite laminated Euler–Bernoulli and Timoshenko beams. International Journal of Engineering Science, 2014. **75**: p. 40-53.

40. Mohammadabadi M., Daneshmehr A., and Homayounfard M., *Size-dependent thermal buckling analysis of micro composite laminated beams using modified couple stress theory.* International Journal of Engineering Science, 2015. **92**: p. 47-62.
41. Chen W.J. and Li X.P., *Size-dependent free vibration analysis of composite laminated Timoshenko beam based on new modified couple stress theory.* Archive of Applied Mechanics, 2013: p. 1-14.
42. Mohammad-Abadi M. and Daneshmehr A., *Modified couple stress theory applied to dynamic analysis of composite laminated beams by considering different beam theories.* International Journal of Engineering Science, 2015. **87**: p. 83-102.
43. Ghadiri M., Zajkani A., and Akbarizadeh M.R., *Thermal effect on dynamics of thin and thick composite laminated microbeams by modified couple stress theory for different boundary conditions.* Applied Physics A, 2016. **122**(12): p. 1023.
44. Thanh C.-L., Phung-Van P., Thai C.H., Nguyen-Xuan H., and Wahab M.A., *Isogeometric analysis of functionally graded carbon nanotube reinforced composite nanoplates using modified couple stress theory.* Composite Structures, 2018. **184**: p. 633-649.
45. Nguyen T.N., Ngo T.D., and Nguyen-Xuan H., *A novel three-variable shear deformation plate formulation: Theory and Isogeometric implementation.* Computer Methods in Applied Mechanics and Engineering, 2017. **326**: p. 376-401.
46. Şimşek M., *Non-linear vibration analysis of a functionally graded Timoshenko beam under action of a moving harmonic load.* Composite Structures, 2010. **92**(10):

p. 2532-2546.

47. Şimşek M., *Static analysis of a functionally graded beam under a uniformly distributed load by Ritz method.* Int J Eng Appl Sci, 2009. **1**(3): p. 1-11.
48. Fakher M. and Hosseini-Hashemi S., *Bending and free vibration analysis of nanobeams by differential and integral forms of nonlocal strain gradient with Rayleigh–Ritz method.* Materials Research Express, 2017. **4**(12): p. 125025.
49. Xu X.-j. and Deng Z.-c., *Variational principles for buckling and vibration of MWCNTs modeled by strain gradient theory.* Applied Mathematics and Mechanics, 2014. **35**(9): p. 1115-1128.
50. Reddy J.N., *Mechanics of laminated composite plates and shells: theory and analysis*. 2004: CRC press.
51. Ilanko S., Monterrubio L., and Mochida Y., *The Rayleigh-Ritz method for structural analysis*. 2015: John Wiley & Sons.
52. Shi G., *A new simple third-order shear deformation theory of plates.* International Journal of Solids and Structures, 2007. **44**(13): p. 4399-4417.
53. Reissner E., *On transverse bending of plates, including the effect of transverse shear deformation.* International Journal of Solids and Structures, 1975. **11**(5): p. 569-573.

Figure Captions

Figure 1. Geometry and coordinate of a laminated composite beam.

Figure 2. Comparison of the critical buckling loads of cross-ply S-S microbeams (MAT I).

Figure 3. Comparison of the fundamental frequencies of cross-ply S-S microbeams (MAT I).

Figure 4. Comparison of displacement and normal stress of $\left(90^0/0^0/90^0\right)$ S-S beams (MAT II).

Figure 5. Effect of MLSP on the displacements of S-S beams (MAT II, $L/h=4$).

Figure 6. Effect of MLSP on the displacements of C-F beams (MAT II, $L/h=4$).

Figure 7. Effect of MLSP on the displacements of C-C beams (MAT II, $L/h=4$).

Figure 8. Effect of MLSP on the displacements of beams with various BCs (MAT II, $L/h=4$).

Figure 9. Effect of MLSP on the distribution of stresses through-thickness of $(0^0/60^0/0^0)$ S-S beams (MAT II, $L/h=4$).

Figure 10. Effect of MLSP on the distribution of stresses through-thickness of $(0^0/60^0)$ S-S beams (MAT II, $L/h=4$).

Figure 11. Effect of MLSP on the natural frequencies of beams with various BCs (MAT III, $L/h=5$).

Figure 12. Effect of MLSP on the critical buckling loads of beams with various BCs (MAT III, $L/h=5$).

Figure 13. The first three mode shapes of $(0^0/45^0/0^0)$ and $(0^0/45^0)$ C-F beams (MAT III, $L/h=5$, $\xi_b=h/4$).

Table Captions

Table 1. Shape functions and essential BC of beams.

Table 2. Material properties of laminated composite beams considered in this study.

Table 3. Convergence studies for ($0^0 / 90^0 / 0^0$) composite beams (MAT I, $L / h = 5$).

Table 4. Displacements of S-S beams (MAT II).

Table 5. Displacements of C-F beams (MAT II).

Table 6. Displacements of C-C beams (MAT II).

Table 7. Fundamental frequencies of ($\theta / -\theta$) beams (MAT III).

Table 8. Fundamental frequencies of ($0^0 / \theta$) beams (MAT III).

Table 9. Critical buckling loads of ($\theta / -\theta$) beams (MAT III).

Table 10. Critical buckling loads of ($0^0 / \theta$) beams (MAT III).

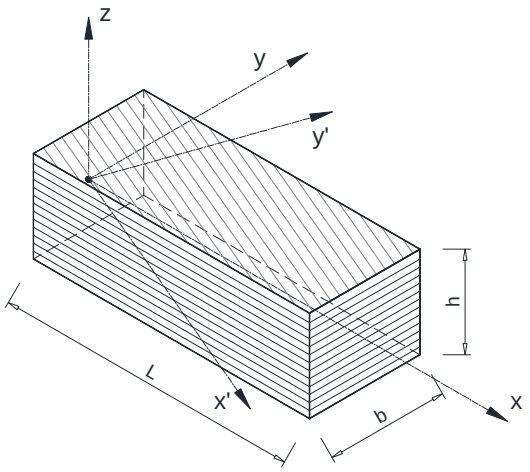

Figure 1. Geometry and coordinate of a laminated composite beam.

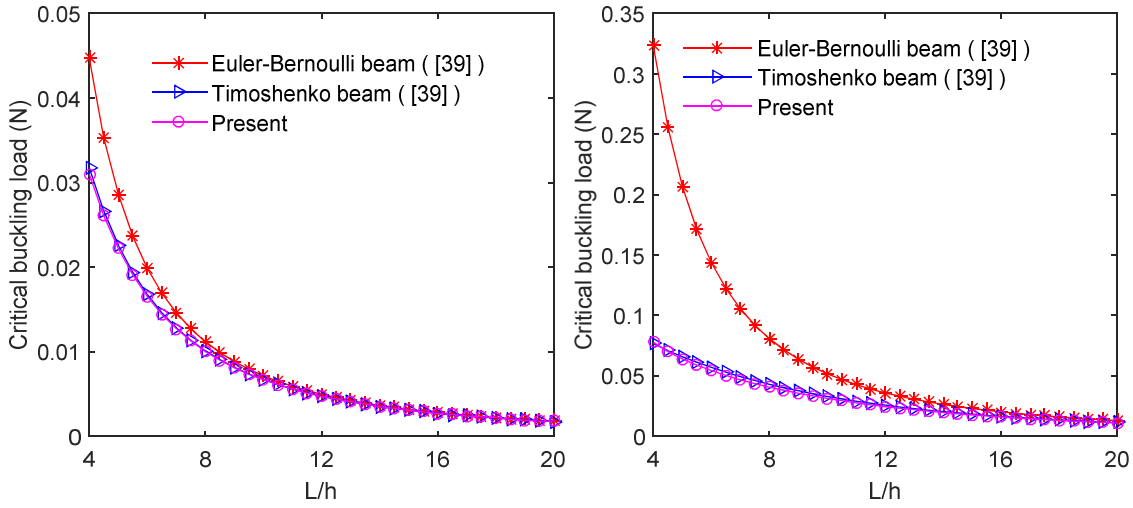

a. $90^0 / 0^0 / 90^0$ b. $0^0 / 90^0 / 0^0$

Figure 2. Comparison of the critical buckling loads of cross-ply S-S microbeams (MAT I).

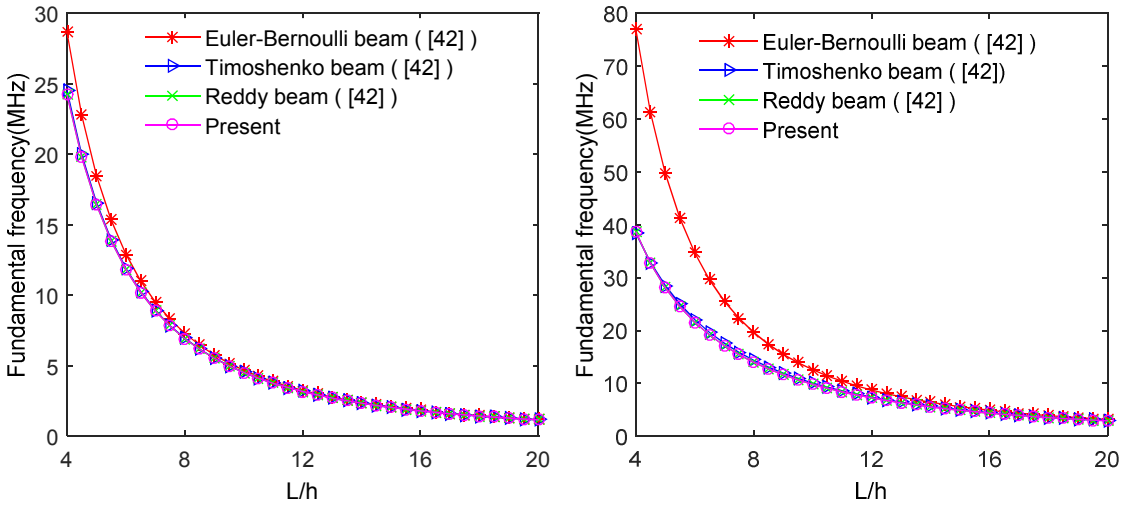

a. $90^0 / 0^0 / 90^0$ b. $0^0 / 90^0 / 0^0$

Figure 3. Comparison of the fundamental frequencies of cross-ply S-S microbeams (MAT I).

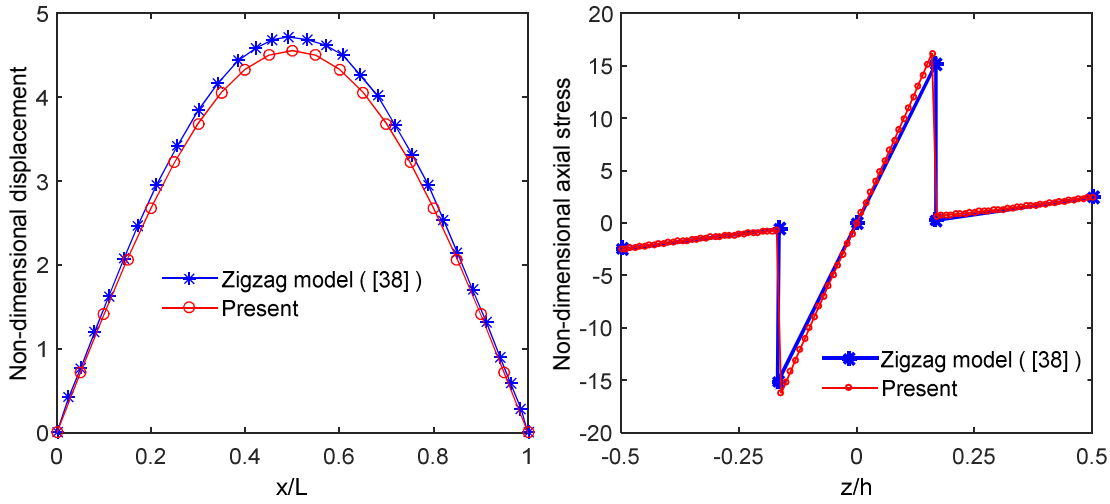

a. Non-dimensional displacement b. Non-dimensional normal stress

Figure 4. Comparison of displacement and normal stress of $\left(90^0/0^0/90^0\right)$ S-S beams (MAT II).

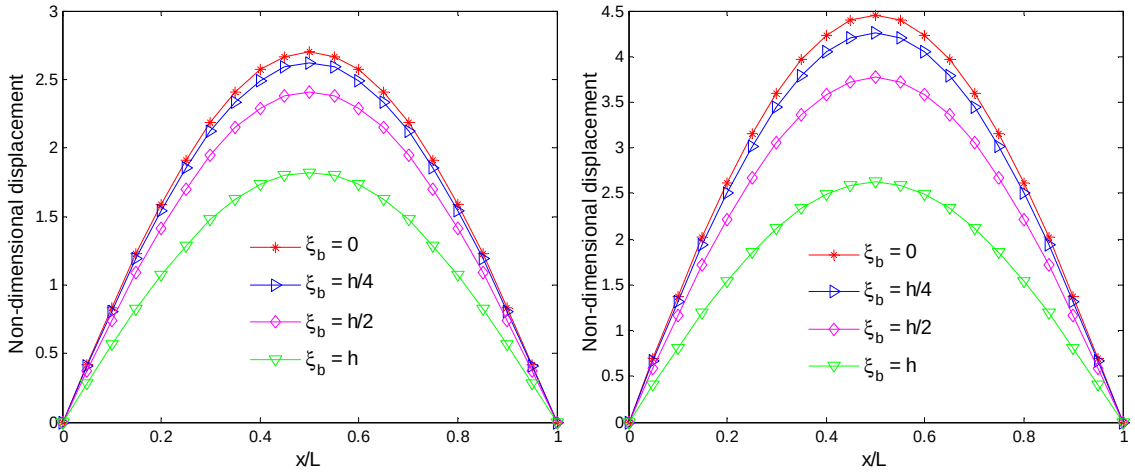

a. $0^0 / 90^0 / 0^0$ b. $0^0 / 90^0$

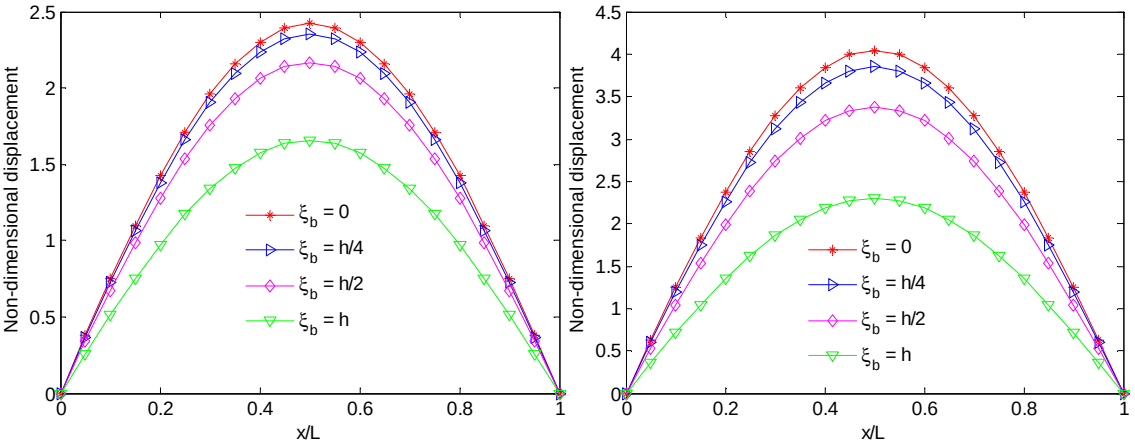

c. $0^0 / 45^0 / 0^0$ d. $0^0 / 45^0$

Figure 5. Effect of MLSP on the displacements of S-S beams (MAT II, $L/h=4$).

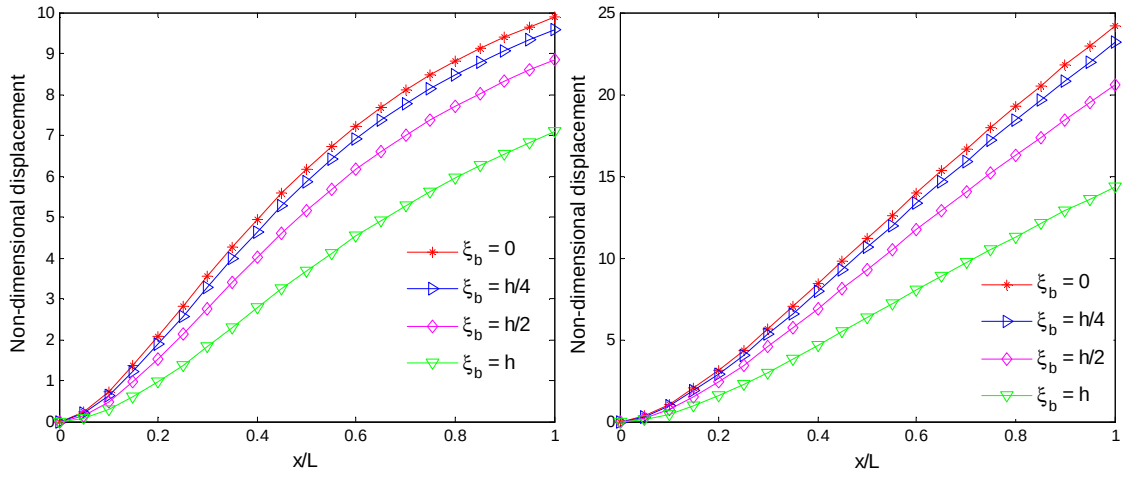

a. $0^0 / 90^0 / 0^0$ b. $0^0 / 90^0$

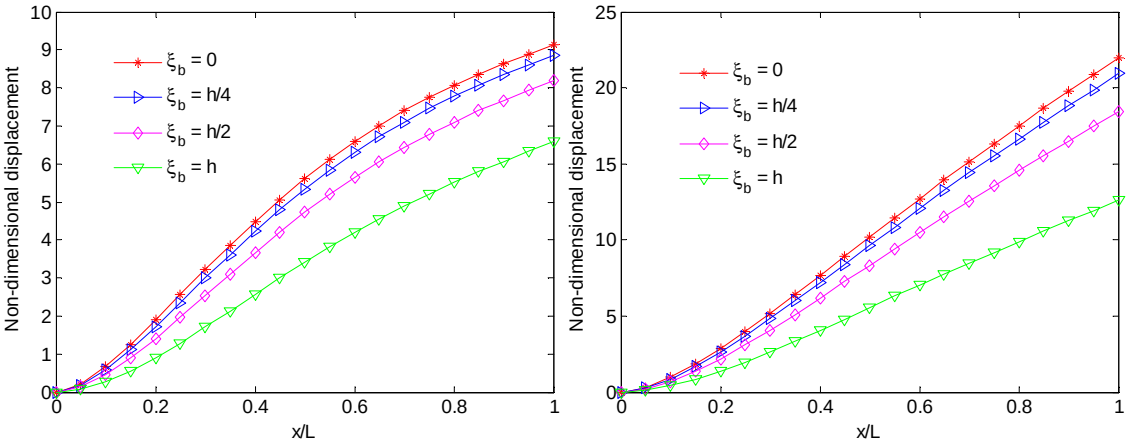

c. $0^0 / 45^0 / 0^0$ d. $0^0 / 45^0$

Figure 6. Effect of MLSP on the displacements of C-F beams (MAT II, $L/h = 4$).

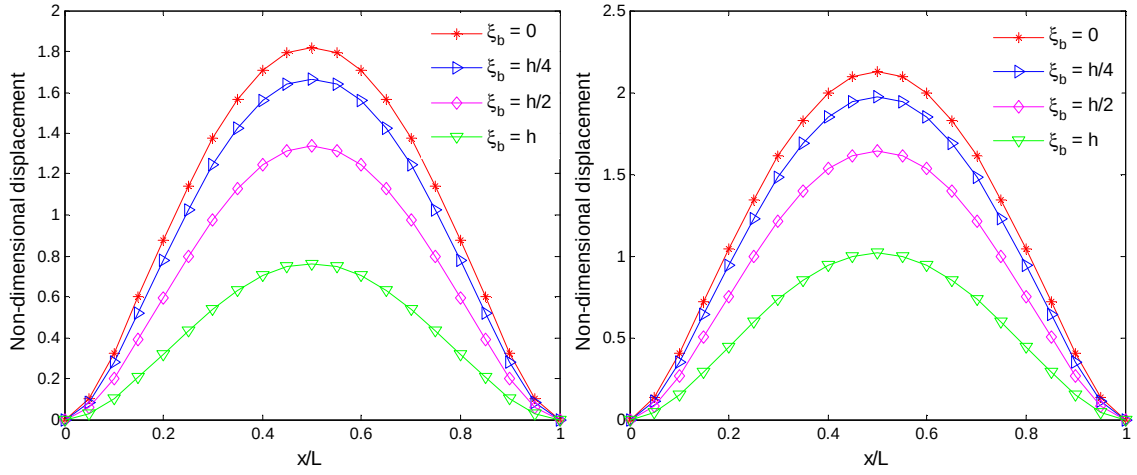

a. $0^0 / 90^0 / 0^0$ b. $0^0 / 90^0$

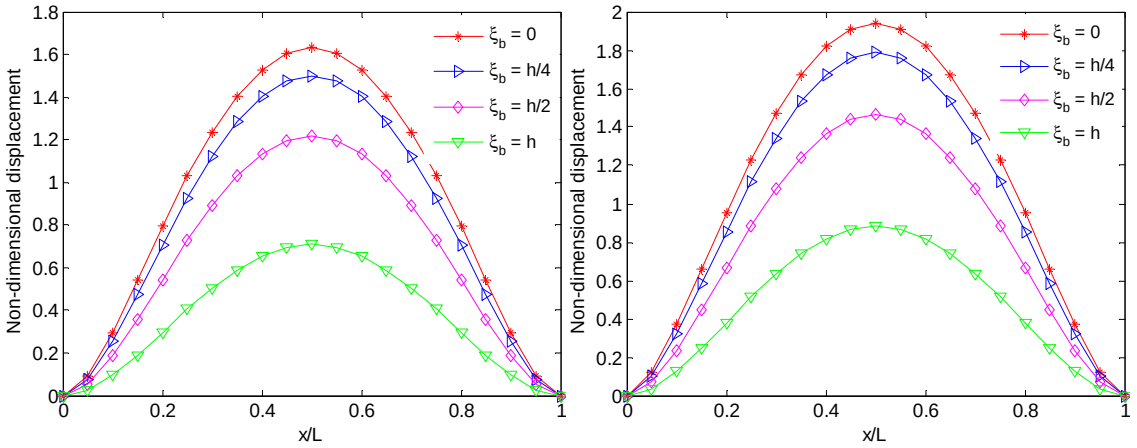

c. $0^0 / 45^0 / 0^0$ d. $0^0 / 45^0$

Figure 7. Effect of MLSP on the displacements of C-C beams (MAT II, $L/h=4$).

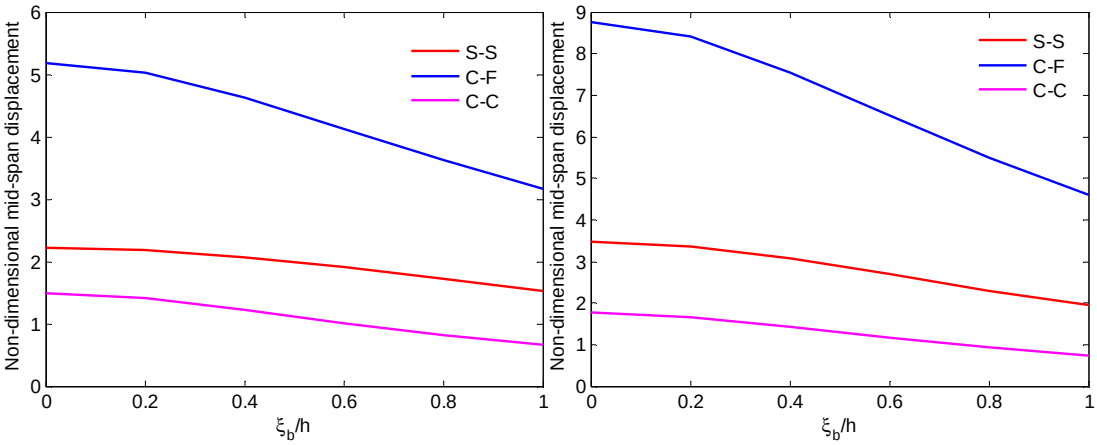

a. $0^0 / 30^0 / 0^0$ b. $0^0 / 30^0$

Figure 8. Effect of MLSP on the displacements of beams with various BCs (MAT II, $L / h = 4$).

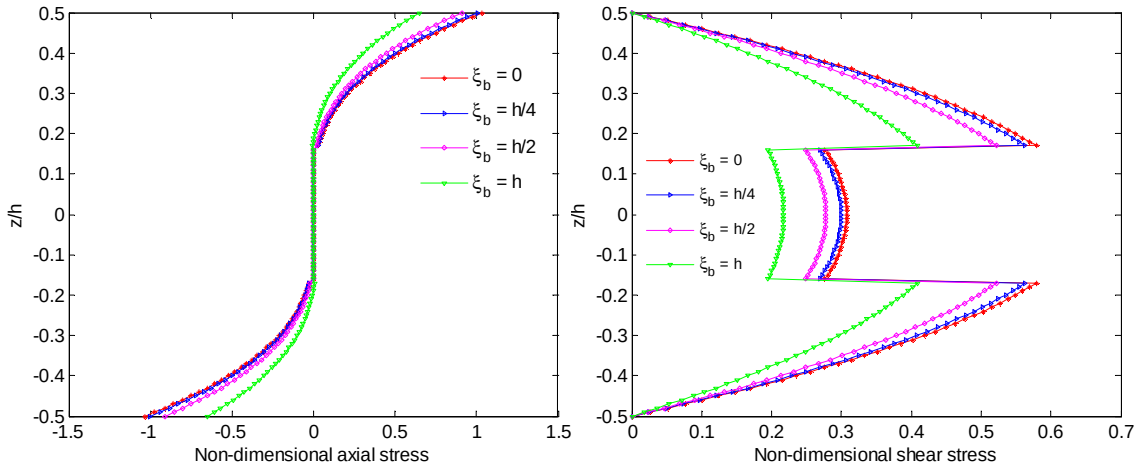

a. $\bar{\sigma}_{xx}$ b. $\bar{\sigma}_{xz}$

Figure 9. Effect of MLSP on the distribution of stresses through-thickness of $(0^0/60^0/0^0)$ S-S beams (MAT II, $L/h=4$).

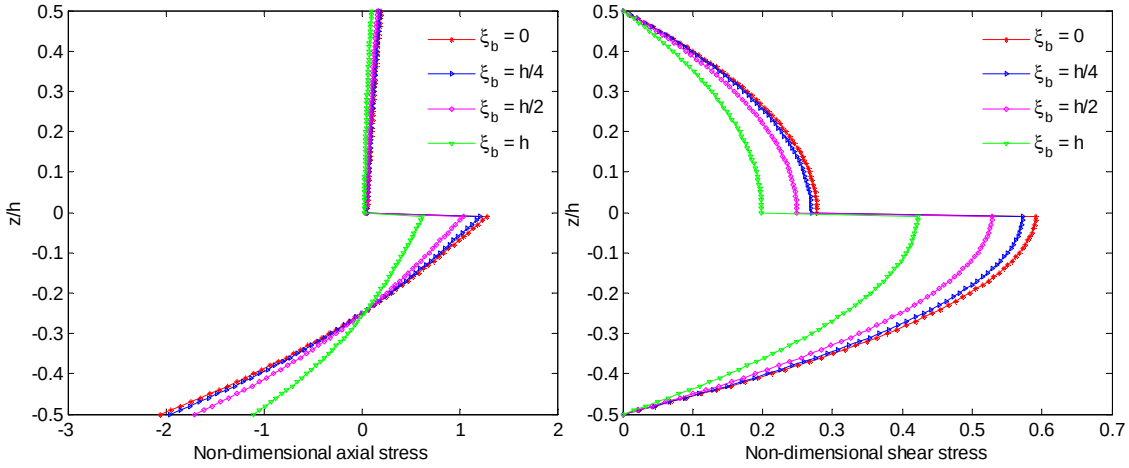

a. $\bar{\sigma}_{xx}$ b. $\bar{\sigma}_{xz}$

Figure 10. Effect of MLSP on the distribution of stresses through-thickness of ($0^0 / 60^0$) S-S beams (MAT II, $L/h = 4$).

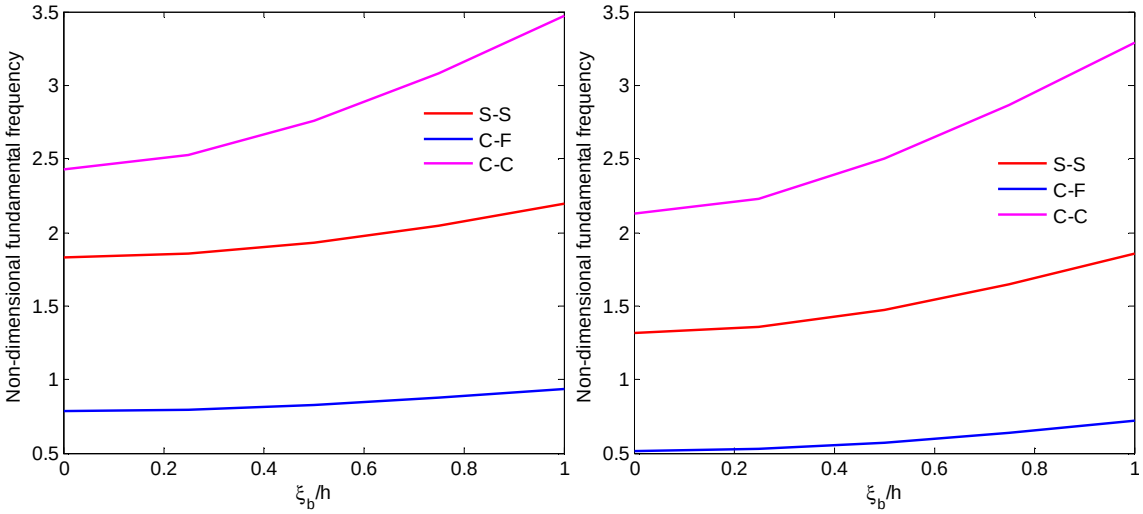

a. $0^0 / 30^0 / 0^0$ b. $0^0 / 30^0$

Figure 11. Effect of MLSP on the natural frequencies of beams with various BCs (MAT III, $L / h = 5$).

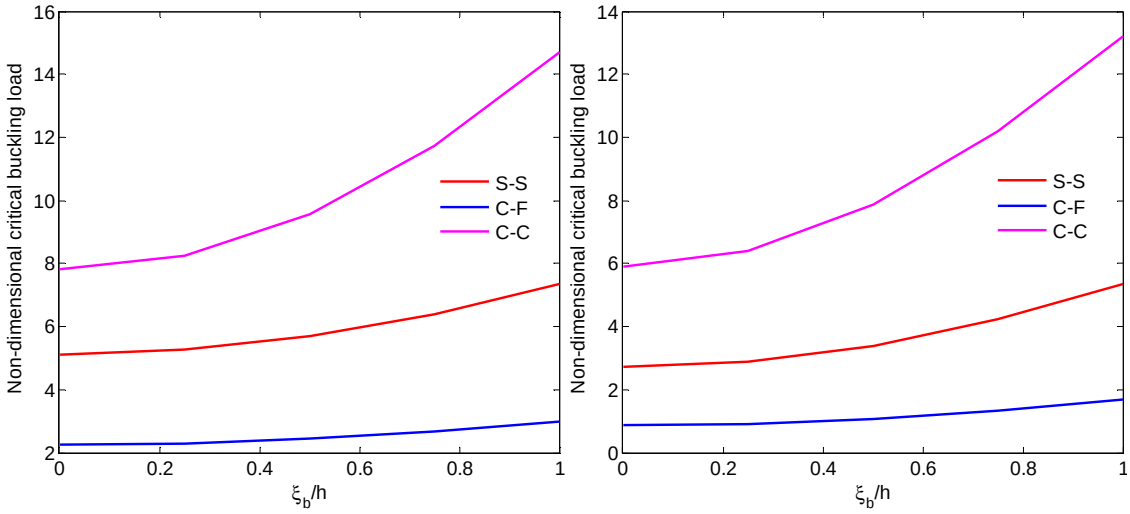

b. $0^0 / 30^0 / 0^0$ b. $0^0 / 30^0$

Figure 12. Effect of MLSP on the critical buckling loads of beams with various BCs (MAT III, $L / h = 5$).

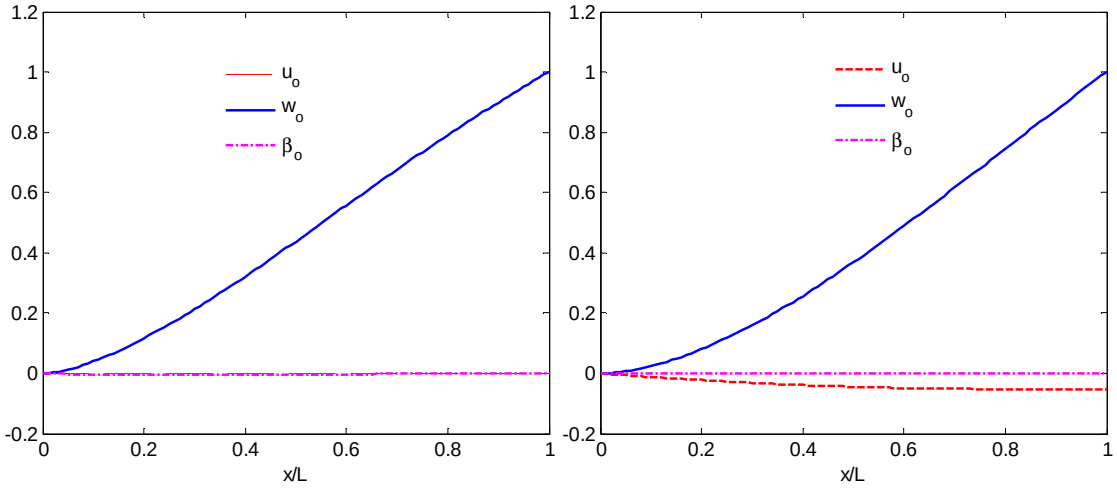

a. $0^0 / 45^0 / 0^0$, $\bar{\omega}_1 = 0.7919$ b. $0^0 / 45^0$, $\bar{\omega}_1 = 0.4805$

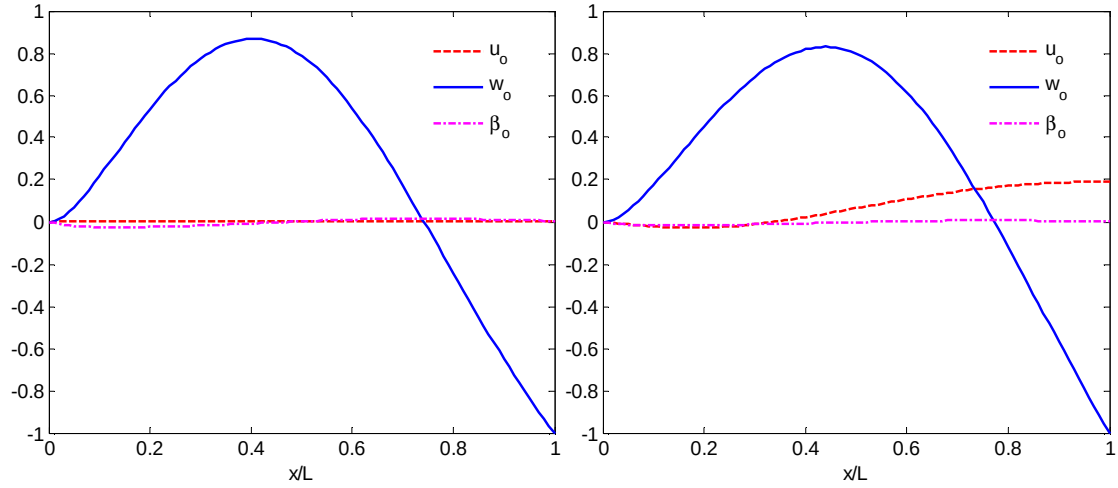

c. $0^0 / 45^0 / 0^0$, $\bar{\omega}_2 = 2.9614$ d. $0^0 / 45^0$, $\bar{\omega}_2 = 2.2643$

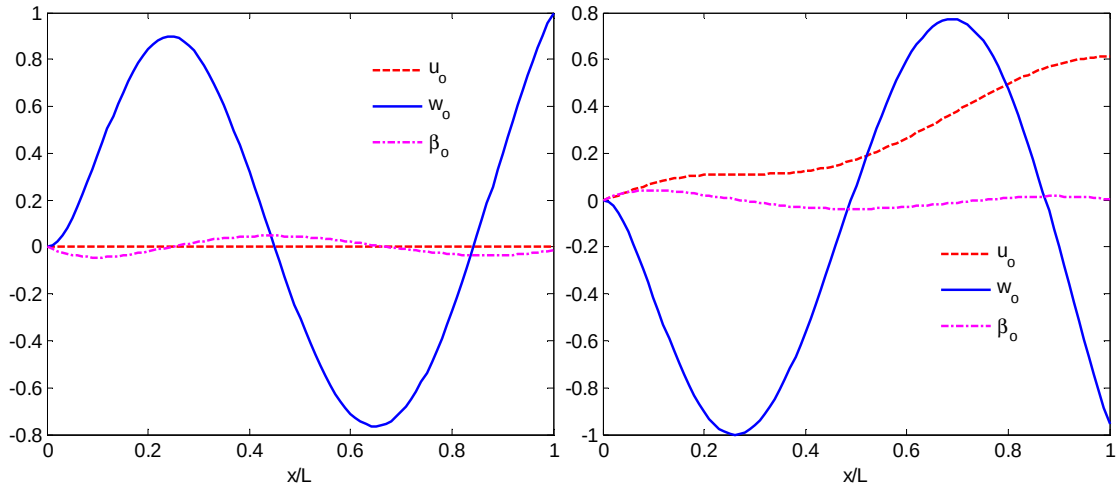

e. $0^0 / 45^0 / 0^0$, $\bar{\omega}_3 = 6.1203$ f. $0^0 / 45^0$, $\bar{\omega}_3 = 5.0419$

Figure 13. The first three mode shapes of ($0^0 / 45^0 / 0^0$) and ($0^0 / 45^0$) C-F beams (MAT III, $L / h = 5$, $\xi_b = h / 4$).

Table 1. Shape functions and essential BC of beams.

BC	$\varphi_j(x)$	x=0	x=L
S-S	$\left(1-e^{\frac{-jx}{L}}\right)\left(1-e^{-j\left(1-\frac{x}{L}\right)}\right)$	$w_0=0$	$w_0=0$
C-F	$\left(1-\frac{jx}{L}-e^{\frac{-jx}{L}}\right)$	$u_0=0, w_0=0,$ $\beta_0=0, w_{0,x}=0$	
C-C	$\left(1-e^{\frac{-jx}{L}}\right)^2\left(1-e^{-j\left(1-\frac{x}{L}\right)}\right)^2$	$u_0=0, w_0=0,$ $\beta_0=0, w_{0,x}=0$	$u_0=0, w_0=0,$ $\beta_0=0, w_{0,x}=0$

Table 2. Material properties of laminated composite beams considered in this study.

Material properties	MAT I [13]	MAT II [38]	MAT III [11]
$E_2=E_3$ (GPa)	*6.98*	10^{-3}	9.65
E_1 (GPa)	$25E_2$	$25E_2$	144.8
$G_{12}=G_{13}$ (GPa)	$0.5E_2$	$0.5E_2$	4.14
G_{23} (GPa)	$0.2E_2$	$0.2E_2$	3.45
ν_{12}	0.25	0.25	0.3
ν_{13}	0.25	0.25	0.3
ν_{23}	0.25	0.25	0.3
h (μm)	4	$2x10^3$	25
b (μm)	8	$1x10^3$	25

Table 3. Convergence studies for ($0^0 / 90^0 / 0^0$) composite beams (MAT I, $L / h = 5$).

BC	ξ_b / h	m				
		2	4	6	8	10
Fundamental frequency						
S-S	0	7.1811	7.1796	7.1796	7.1796	7.1796
	1	8.4006	8.3979	8.3979	8.3979	8.3979
C-F	0	3.3711	3.3163	3.3111	3.3108	3.3108
	1	3.8675	3.8433	3.8416	3.8415	3.8415
C-C	0	9.0547	9.0359	9.0359	9.0359	9.0359
	1	13.0536	13.0530	13.0530	13.0530	13.0530
Critical buckling load						
S-S	0	5.2373	5.2354	5.2354	5.2354	5.2354
	1	7.1639	7.1599	7.1599	7.1599	7.1599
C-F	0	2.9459	2.8950	2.8945	2.8945	2.8945
	1	3.3750	3.5088	3.5082	3.5082	3.5082
C-C	0	7.0582	7.0564	7.0564	7.0564	7.0564
	1	13.7654	13.7555	13.7555	13.7555	13.7555
Mid-span displacement						
S-S	0	2.4216	2.4144	2.4141	2.4141	2.4141
	1	1.7870	1.7827	1.7826	1.7826	1.7826
C-F	0	6.1552	6.8006	6.8309	6.8301	6.8306
	1	4.3796	4.6111	4.6061	4.6060	4.6061
C-C	0	1.5127	1.5375	1.5378	1.5378	1.5378
	1	0.7551	0.7556	0.7556	0.7556	0.7556

Table 4. Displacements of S-S beams (MAT II).

L/h	Lay-ups	θ	Vo et al. [1]	Present			
			$(\xi_b = 0)$	$\xi_b = 0$	$\xi_b = h/4$	$\xi_b = h/2$	$\xi_b = h$
5	$0^0/\theta/0^0$	0^0	1.7930	1.8021	1.7622	1.6523	1.3240
		15^0	1.8626	1.8718	1.8305	1.7166	1.3756
		30^0	2.0140	2.0233	1.9799	1.8596	1.4959
		45^0	2.1762	2.1854	2.1398	2.0130	1.6251
		60^0	2.3030	2.3122	2.2642	2.1303	1.7197
		75^0	2.3796	2.3888	2.3385	2.1981	1.7688
		90^0	2.4049	2.4141	2.3627	2.2195	1.7826
	$0^0/\theta$	0^0	1.7930	1.8021	1.7622	1.6523	1.3240
		15^0	2.5763	2.5890	2.4967	2.2568	1.6430
		30^0	3.6634	3.6836	3.5127	3.0870	2.1039
		45^0	4.3135	4.3420	4.1490	3.6647	2.5254
		60^0	4.6135	4.6511	4.4605	3.9759	2.7980
		75^0	4.7162	4.7627	4.5699	4.0787	2.8793
		90^0	4.7346	4.7852	4.5895	4.0917	2.8814
10	$0^0/\theta/0^0$	0^0	0.9222	0.9236	0.9086	0.8664	0.7320
		15^0	0.9529	0.9543	0.9390	0.8960	0.7584
		30^0	0.9946	0.9961	0.9814	0.9398	0.8047
		45^0	1.0370	1.0385	1.0245	0.9848	0.8531
		60^0	1.0700	1.0715	1.0577	1.0186	0.8875
		75^0	1.0900	1.0914	1.0774	1.0376	0.9044
		90^0	1.0965	1.0980	1.0838	1.0436	0.9089
	$0^0/\theta$	0^0	0.9222	0.9236	0.9086	0.8664	0.7320
		15^0	1.6861	1.6890	1.6364	1.4973	1.1213
		30^0	2.7402	2.7482	2.6290	2.3274	1.6024
		45^0	3.3370	3.3515	3.2101	2.8506	1.9763
		60^0	3.5871	3.6094	3.4687	3.1064	2.1985
		75^0	3.6562	3.6865	3.5445	3.1785	2.2568
		90^0	3.6626	3.6966	3.5529	3.1829	2.2545
50	$0^0/\theta/0^0$	0^0	0.6370	0.6370	0.6276	0.6008	0.5135
		15^0	0.6554	0.6555	0.6460	0.6190	0.5304
		30^0	0.6608	0.6609	0.6523	0.6279	0.5462
		45^0	0.6634	0.6634	0.6558	0.6343	0.5605
		60^0	0.6650	0.6650	0.6580	0.6380	0.5687
		75^0	0.6658	0.6659	0.6590	0.6392	0.5707
		90^0	0.6651	0.6661	0.6592	0.6394	0.5706
	$0^0/\theta$	0^0	0.6370	0.6370	0.6276	0.6008	0.5135
		15^0	1.3966	1.3975	1.3556	1.2437	0.9351
		30^0	2.4406	2.4458	2.3415	2.0759	1.4283
		45^0	3.0200	3.0313	2.9050	2.5823	1.7881
		60^0	3.2540	3.2727	3.1465	2.8204	1.9940
		75^0	3.3121	3.3385	3.2114	2.8822	2.0444
		90^0	3.3147	3.3446	3.2161	2.8836	2.0403

Table 5. Displacements of C-F beams (MAT II).

L/h	Lay-ups	θ	Vo et al. [1]	Present			
			($\xi_b = 0$)	$\xi_b = 0$	$\xi_b = h/4$	$\xi_b = h/2$	$\xi_b = h$
5	$0^0/\theta/0^0$	0^0	5.2774	5.2572	5.0746	4.6404	3.5800
		15^0	5.4898	5.4690	5.2754	4.8196	3.7153
		30^0	5.8804	5.8586	5.6504	5.1624	3.9877
		45^0	6.2879	6.2654	6.0427	5.5219	4.2748
		60^0	6.6029	6.5800	6.3435	5.7916	4.4792
		75^0	6.7919	6.7688	6.5206	5.9429	4.5794
		90^0	6.8541	6.8309	6.5778	5.9896	4.6061
	$0^0/\theta$	0^0	5.2774	5.2572	5.0746	4.6404	3.5800
		15^0	8.0005	7.9914	7.6295	6.7802	4.8235
		30^0	11.6830	11.7047	11.0919	9.6451	6.4689
		45^0	13.8390	13.8972	13.2173	11.5765	7.8662
		60^0	14.8020	14.8997	14.2305	12.5869	8.7400
		75^0	15.1080	15.2447	14.5676	12.9015	8.9857
		90^0	15.1540	15.3084	14.6211	12.9334	8.9841
10	$0^0/\theta/0^0$	0^0	2.9663	2.9653	2.9082	2.7550	2.2981
		15^0	3.0653	3.0641	3.0053	2.8480	2.3795
		30^0	3.1828	3.1817	3.1236	2.9687	2.5060
		45^0	3.2992	3.2983	3.2412	3.0895	2.6354
		60^0	3.3889	3.3882	3.3307	3.1786	2.7245
		75^0	3.4428	3.4423	3.3832	3.2276	2.7653
		90^0	3.4605	3.4601	3.4001	3.2425	2.7753
	$0^0/\theta$	0^0	2.9663	2.9653	2.9082	2.7550	2.2981
		15^0	5.5712	5.5740	5.3917	4.9165	3.6591
		30^0	9.1499	9.1716	8.7662	7.7464	5.3131
		45^0	11.1650	11.2129	10.7332	9.5182	6.5783
		60^0	12.0020	12.0801	11.6027	10.3782	7.3237
		75^0	12.2260	12.3353	11.8537	10.6162	7.5158
		90^0	12.2440	12.3673	11.8797	10.6288	7.5061
50	$0^0/\theta/0^0$	0^0	2.1602	2.1598	2.1278	2.0372	1.7408
		15^0	2.2228	2.2224	2.1901	2.0986	1.7981
		30^0	2.2405	2.2401	2.2110	2.1282	1.8512
		45^0	2.2483	2.2479	2.2223	2.1491	1.8990
		60^0	2.2531	2.2526	2.2289	2.1610	1.9262
		75^0	2.2557	2.2551	2.2318	2.1648	1.9327
		90^0	2.2565	2.2559	2.2325	2.1652	1.9322
	$0^0/\theta$	0^0	2.1602	2.1598	2.1278	2.0372	1.7408
		15^0	4.7429	4.7456	4.6033	4.2232	3.1753
		30^0	8.2916	8.3096	7.9551	7.0528	4.8524
		45^0	10.2600	10.3000	9.8708	8.7742	6.0756
		60^0	11.0540	11.1202	10.6915	9.5833	6.7754
		75^0	11.2500	11.3437	10.9118	9.7932	6.9463
		90^0	11.2580	11.3645	10.9277	9.7980	6.9325

Table 6. Displacements of C-C beams (MAT II).

L/h	Lay-ups	θ	Vo et al. [1]	Present			
			($\xi_b = 0$)	$\xi_b = 0$	$\xi_b = h/4$	$\xi_b = h/2$	$\xi_b = h$
5	$0^0/\theta/0^0$	0^0	1.0998	1.0908	1.0239	0.8756	0.5709
		15^0	1.1537	1.1442	1.0723	0.9145	0.5937
		30^0	1.2670	1.2569	1.1767	1.0008	0.6442
		45^0	1.3856	1.3751	1.2865	1.0915	0.6971
		60^0	1.4766	1.4658	1.3699	1.1587	0.7339
		75^0	1.5309	1.5200	1.4186	1.1956	0.7513
		90^0	1.5487	1.5378	1.4341	1.2067	0.7556
	$0^0/\theta$	0^0	1.0998	1.0908	1.0239	0.8756	0.5709
		15^0	1.3165	1.3083	1.2106	1.0068	0.6263
		30^0	1.5755	1.5707	1.4497	1.1960	0.7345
		45^0	1.7547	1.7528	1.6317	1.3684	0.8650
		60^0	1.8575	1.8582	1.7414	1.4806	0.9599
		75^0	1.9060	1.9091	1.7904	1.5244	0.9910
		90^0	1.9193	1.9236	1.8025	1.5320	0.9927
10	$0^0/\theta/0^0$	0^0	0.3968	0.3957	0.3831	0.3527	0.2750
		15^0	0.4130	0.4119	0.3986	0.3667	0.2875
		30^0	0.4469	0.4457	0.4315	0.3973	0.3104
		45^0	0.4828	0.4816	0.4664	0.4299	0.3369
		60^0	0.5108	0.5096	0.4934	0.4547	0.3563
		75^0	0.5277	0.5264	0.5095	0.4689	0.3662
		90^0	0.5332	0.5319	0.5147	0.4734	0.3690
	$0^0/\theta$	0^0	0.3968	0.3957	0.3831	0.3527	0.2750
		15^0	0.5584	0.5581	0.5335	0.4751	0.3391
		30^0	0.7783	0.7799	0.7392	0.6431	0.4326
		45^0	0.9107	0.9142	0.8695	0.7618	0.5191
		60^0	0.9726	0.9782	0.9343	0.8266	0.5754
		75^0	0.9943	1.0019	0.9575	0.8481	0.5923
		90^0	0.9983	1.0068	0.9617	0.8509	0.5927
50	$0^0/\theta/0^0$	0^0	0.1367	0.1367	0.1346	0.1287	0.1097
		15^0	0.1408	0.1408	0.1387	0.1327	0.1134
		30^0	0.1431	0.1430	0.1411	0.1356	0.1176
		45^0	0.1449	0.1448	0.1431	0.1382	0.1215
		60^0	0.1462	0.1461	0.1445	0.1399	0.1240
		75^0	0.1470	0.1469	0.1453	0.1407	0.1249
		90^0	0.1472	0.1472	0.1456	0.1409	0.1251
	$0^0/\theta$	0^0	0.1367	0.1367	0.1346	0.1287	0.1097
		15^0	0.2887	0.2889	0.2802	0.2569	0.1930
		30^0	0.4974	0.4989	0.4776	0.4233	0.2913
		45^0	0.6137	0.6166	0.5909	0.5251	0.3637
		60^0	0.6608	0.6654	0.6397	0.5733	0.4054
		75^0	0.6727	0.6790	0.6530	0.5860	0.4157
		90^0	0.6733	0.6803	0.6541	0.5864	0.4150

Table 7. Fundamental frequencies of ($\theta / -\theta$) beams (MAT III).

BC	L/h	θ	Chen et al. [7]	Vo et al. [2]	Present			
			($\xi_b = 0$)	($\xi_b = 0$)	$\xi_b = 0$	$\xi_b = h/4$	$\xi_b = h/2$	$\xi_b = h$
S-S	5	0^0	-	-	1.8492	1.8766	1.9559	2.2383
		15^0	-	-	1.3355	1.3794	1.5020	1.9008
		30^0	-	-	0.9185	0.9727	1.1181	1.5555
		45^0	-	-	0.7484	0.7903	0.9037	1.2510
		60^0	-	-	0.6912	0.7121	0.7712	0.9700
		75^0	-	-	0.6847	0.6899	0.7054	0.7641
		90^0	-	-	0.6886	0.6886	0.6886	0.6886
	15	0^0	-	-	2.6494	2.6785	2.7637	3.0789
		15^0	-	-	1.5794	1.6268	1.7610	2.2150
		30^0	-	-	0.9986	1.0556	1.2105	1.6914
		45^0	-	-	0.7958	0.8395	0.9585	1.3310
		60^0	-	-	0.7310	0.7527	0.8143	1.0239
		75^0	-	-	0.7245	0.7300	0.7461	0.8072
		90^0	-	-	0.7295	0.7295	0.7295	0.7295
C-F	5	0^0	-	-	0.7956	0.8083	0.8427	0.9580
		15^0	-	-	0.5230	0.5403	0.5876	0.7427
		30^0	-	-	0.3435	0.3636	0.4177	0.5829
		45^0	-	-	0.2764	0.2918	0.3334	0.4626
		60^0	-	-	0.2545	0.2621	0.2837	0.3569
		75^0	-	-	0.2521	0.2541	0.2597	0.2812
		90^0	-	-	0.2538	0.2538	0.2538	0.2538
	15	0^0	-	-	0.9803	0.9910	1.0224	1.1386
		15^0	-	-	0.5706	0.5876	0.6360	0.8003
		30^0	-	-	0.3580	0.3784	0.4339	0.6067
		45^0	-	-	0.2848	0.3004	0.3430	0.4765
		60^0	-	-	0.2615	0.2692	0.2913	0.3663
		75^0	-	-	0.2592	0.2611	0.2669	0.2887
		90^0	-	-	0.2610	0.2610	0.2610	0.2610
C-C	5	0^0	-	2.4448	2.4605	2.5572	2.8013	3.5424
		15^0	-	2.0785	2.0843	2.2077	2.5020	3.3382
		30^0	-	1.6668	1.6642	1.7942	2.1076	2.9612
		45^0	-	1.4409	1.4347	1.5322	1.7766	2.4692
		60^0	-	1.3546	1.3452	1.3944	1.5252	1.9389
		75^0	-	1.3428	1.3304	1.3431	1.3793	1.5092
		90^0	-	1.3477	1.3342	1.3342	1.3342	1.3342
	15	0^0	4.8575	4.9004	4.8968	4.9697	5.1701	5.8566
		15^0	3.6113	3.2912	3.2878	3.3948	3.6903	4.6565
		30^0	2.3016	2.1832	2.1802	2.3077	2.6502	3.6930
		45^0	1.8145	1.7621	1.7585	1.8564	2.1215	2.9403
		60^0	1.6686	1.6249	1.6201	1.6688	1.8065	2.2718
		75^0	1.6200	1.6117	1.6053	1.6175	1.6536	1.7904
		90^0	1.6237	1.6227	1.6153	1.6153	1.6153	1.6153

Table 8. Fundamental frequencies of ($0^0 / \theta$) beams (MAT III).

BC	L/h	θ	Chen et al. [7]	Vo et al. [2]	Present			
			($\xi_b = 0$)	($\xi_b = 0$)	$\xi_b = 0$	$\xi_b = h/4$	$\xi_b = h/2$	$\xi_b = h$
S-S	5	0^0	-	-	1.8492	1.8766	1.9559	2.2383
		15^0	-	-	1.5757	1.6111	1.7119	2.0557
		30^0	-	-	1.3198	1.3612	1.4771	1.8575
		45^0	-	-	1.2118	1.2510	1.3608	1.7205
		60^0	-	-	1.1754	1.2096	1.3061	1.6275
		75^0	-	-	1.1703	1.2006	1.2866	1.5776
		90^0	-	-	1.1722	1.2011	1.2833	1.5631
	15	0^0	-	-	2.6494	2.6785	2.7637	3.0789
		15^0	-	-	1.9962	2.0348	2.1461	2.5404
		30^0	-	-	1.5437	1.5886	1.7160	2.1489
		45^0	-	-	1.3827	1.4250	1.5449	1.9501
		60^0	-	-	1.3329	1.3698	1.4749	1.8346
		75^0	-	-	1.3278	1.3605	1.4541	1.7786
		90^0	-	-	1.3314	1.3626	1.4521	1.7639
C-F	5	0^0	-	-	0.7956	0.8083	0.8427	0.9580
		15^0	-	-	0.6396	0.6542	0.6946	0.8305
		30^0	-	-	0.5140	0.5300	0.5745	0.7219
		45^0	-	-	0.4656	0.4805	0.5223	0.6604
		60^0	-	-	0.4500	0.4631	0.4997	0.6226
		75^0	-	-	0.4482	0.4597	0.4924	0.6035
		90^0	-	-	0.4492	0.4602	0.4914	0.5983
	15	0^0	-	-	0.9803	0.9910	1.0224	1.1386
		15^0	-	-	0.7266	0.7406	0.7809	0.9245
		30^0	-	-	0.5571	0.5733	0.6192	0.7758
		45^0	-	-	0.4979	0.5131	0.5562	0.7024
		60^0	-	-	0.4797	0.4929	0.5307	0.6604
		75^0	-	-	0.4779	0.4896	0.5233	0.6402
		90^0	-	-	0.4792	0.4904	0.5226	0.6349
C-C	5	0^0	-	2.4448	2.4605	2.5572	2.8013	3.5424
		15^0	-	2.2820	2.2928	2.4000	2.6651	3.4469
		30^0	-	2.1200	2.1245	2.2319	2.5015	3.2864
		45^0	-	2.0343	2.0347	2.1313	2.3785	3.1065
		60^0	-	1.9999	1.9968	2.0804	2.2975	2.9511
		75^0	-	1.9928	1.9866	2.0609	2.2558	2.8531
		90^0	-	1.9935	1.9860	2.0570	2.2441	2.8211
	15	0^0	4.8575	4.9004	4.8968	4.9697	5.1701	5.8566
		15^0	4.1899	3.9967	3.9915	4.0805	4.3278	5.1646
		30^0	3.3548	3.2489	3.2406	3.3408	3.6201	4.5414
		45^0	2.9814	2.9575	2.9457	3.0398	3.3027	4.1705
		60^0	2.9491	2.8669	2.8500	2.9320	3.1629	3.9364
		75^0	2.8002	2.8615	2.8383	2.9109	3.1167	3.8162
		90^0	2.8012	2.8709	2.8443	2.9136	3.1103	3.7828

Table 9. Critical buckling loads of ($\theta / -\theta$) beams (MAT III).

BC	L/h	θ	Present			
			$\xi_b = 0$	$\xi_b = h/4$	$\xi_b = h/2$	$\xi_b = h$
S-S	5	0^0	5.2343	5.3899	5.8533	7.6577
		15^0	2.7563	2.9394	3.4823	5.5608
		30^0	1.3140	1.4730	1.9443	3.7485
		45^0	0.8745	0.9750	1.2739	2.4340
		60^0	0.7464	0.7921	0.9287	1.4671
		75^0	0.7324	0.7436	0.7773	0.9116
		90^0	0.7408	0.7408	0.7408	0.7408
	15	0^0	10.7087	10.9449	11.6521	14.4607
		15^0	3.8077	4.0394	4.7333	7.4883
		30^0	1.5224	1.7013	2.2370	4.3671
		45^0	0.9669	1.0759	1.4027	2.7046
		60^0	0.8160	0.8651	1.0124	1.6007
		75^0	0.8015	0.8136	0.8499	0.9949
		90^0	0.8125	0.8125	0.8125	0.8125
C-F	5	0^0	2.2972	2.3501	2.5082	3.1323
		15^0	0.8982	0.9535	1.1187	1.7695
		30^0	0.3714	0.4152	0.5462	1.0633
		45^0	0.2378	0.2647	0.3451	0.6643
		60^0	0.2011	0.2132	0.2496	0.3945
		75^0	0.1975	0.2005	0.2094	0.2452
		90^0	0.2001	0.2001	0.2001	0.2001
	15	0^0	2.9724	3.0375	3.2298	3.9974
		15^0	0.9874	1.0471	1.2262	1.9411
		30^0	0.3864	0.4316	0.5675	1.1099
		45^0	0.2441	0.2716	0.3541	0.6835
		60^0	0.2058	0.2182	0.2553	0.4037
		75^0	0.2022	0.2052	0.2144	0.2509
		90^0	0.2050	0.2050	0.2050	0.2050
C-C	5	0^0	7.9859	8.4589	9.8645	15.3013
		15^0	5.7638	6.2940	7.8501	13.6154
		30^0	3.6046	4.1007	5.5445	10.7495
		45^0	2.6489	2.9785	3.9448	7.5065
		60^0	2.3211	2.4736	2.9260	4.6610
		75^0	2.2712	2.3087	2.4210	2.8651
		90^0	2.2856	2.2856	2.2856	2.2856
	15	0^0	30.6893	31.4445	33.6981	42.5424
		15^0	13.3197	14.1548	16.6432	26.3519
		30^0	5.7473	6.4294	8.4636	16.4222
		45^0	3.7201	4.1423	5.4039	10.3774
		60^0	3.1536	3.3446	3.9166	6.1887
		75^0	3.0964	3.1434	3.2843	3.8472
		90^0	3.1360	3.1360	3.1360	3.1360

Table 10. Critical buckling loads of (0^0 / θ) beams (MAT III).

BC	L/h	θ	Present			
			$\xi_b = 0$	$\xi_b = h/4$	$\xi_b = h/2$	$\xi_b = h$
S-S	5	0^0	5.2343	5.3899	5.8533	7.6577
		15^0	3.8272	4.0001	4.5137	6.4925
		30^0	2.7128	2.8843	3.3929	5.3424
		45^0	2.2976	2.4476	2.8924	4.6030
		60^0	2.1645	2.2915	2.6688	4.1269
		75^0	2.1456	2.2574	2.5899	3.8793
		90^0	2.1523	2.2589	2.5763	3.8086
	15	0^0	10.7087	10.9449	11.6521	14.4607
		15^0	6.0852	6.3225	7.0331	9.8541
		30^0	3.6429	3.8579	4.5015	7.0582
		45^0	2.9240	3.1057	3.6502	5.8149
		60^0	2.7174	2.8700	3.3273	5.1471
		75^0	2.6967	2.8311	3.2340	4.8381
		90^0	2.7115	2.8400	3.2250	4.7581
C-F	5	0^0	2.2972	2.3501	2.5082	3.1323
		15^0	1.3920	1.4473	1.6127	2.2644
		30^0	0.8641	0.9156	1.0693	1.6752
		45^0	0.7010	0.7448	0.8759	1.3934
		60^0	0.6531	0.6900	0.8004	1.2367
		75^0	0.6480	0.6805	0.7777	1.1627
		90^0	0.6513	0.6823	0.7752	1.1431
	15	0^0	2.9734	3.0375	3.2298	3.9974
		15^0	1.6113	1.6735	1.8600	2.6045
		30^0	0.9412	0.9965	1.1623	1.8241
		45^0	0.7503	0.7968	0.9362	1.4931
		60^0	0.6961	0.7351	0.8521	1.3192
		75^0	0.6909	0.7253	0.8283	1.2399
		90^0	0.6949	0.7278	0.8263	1.2196
C-C	5	0^0	7.9859	8.4589	9.8645	15.3013
		15^0	6.9492	7.4489	8.9245	14.5077
		30^0	5.9147	6.4082	7.8569	13.2243
		45^0	5.3999	5.8359	7.1152	11.8512
		60^0	5.1933	5.5641	6.6547	10.7226
		75^0	5.1398	5.4661	6.4278	10.0403
		90^0	5.1373	5.4483	6.3659	9.8223
	15	0^0	30.6893	31.4445	33.6981	42.5424
		15^0	19.9100	20.7265	23.1605	32.6737
		30^0	12.9047	13.6837	16.0053	25.0737
		45^0	10.6070	11.2768	13.2746	21.0980
		60^0	9.9157	10.4806	12.1667	18.7882
		75^0	9.8354	10.3328	11.8183	17.6633
		90^0	9.8793	10.3542	11.7730	17.3589